White Noise Responsiveness of an AlN Piezoelectric MEMS Cantilever Vibration Energy Harvester

Journal of Physics: Conference Series **557** (2014) 012037 doi:10.1088/1742-6596/557/1/012037

White Noise Responsiveness of an AlN Piezoelectric MEMS Cantilever Vibration Energy Harvester

Y Jia and A A Seshia

Nanoscience Centre, University Cambridge, Cambridge, CB3 0FF, UK

E-mail: yj252@cam.ac.uk; aas41@cam.ac.uk

Abstract. This paper reports the design, analysis and experimental characterisation of a piezoelectric MEMS cantilever vibration energy harvester, the enhancement of its power output by adding various values of end mass, as well as assessing the responsiveness towards white noise. Devices are fabricated using a 0.5 μm AlN on 10 μm doped Si process. Cantilevers with 5 mm length and 2 mm width were tested at either unloaded condition (MC0: f_n 577 Hz) or subjected to estimated end masses of 2 mg (MC2: f_n 129 Hz) and 5 mg (MC5: f_n 80 Hz). While MC0 was able to tolerate a higher drive acceleration prior to saturation (7 g with 0.7 μW), MC5 exhibited higher peak power attainable at a lower input vibration (2.56 μW at 3 ms^{-2}). MC5 was also subjected to band-limited (10 Hz to 2 kHz) white noise vibration, where the power response was only a fraction of its resonant counterpart for the same input: peak instantaneous power >1 μW was only attainable beyond 2 g of white noise, whereas single frequency resonant response only required 2.5 ms^{-2}. Both the first resonant response and the band-limited white noise response were also compared to a numerical model, showing close agreements.

1. Introduction

Amongst the various designs for piezoelectric vibration energy harvesting, cantilever-based topologies have been the most popular [1] due to simplicity of design and its ability to accumulate strain-induced electrical charges near its clamped end and room to accommodate a proof mass near its less strained free end. MEMS iterations of these piezoelectric cantilever harvesters have also been demonstrated in the literature for at least over half a decade [2].

The inclusion of an end mass has been shown, both through simulation and experiment, to drastically improve the power response of the harvester [3] compared to a plain cantilever beam. However, most of these previous studies omit an analysis on the response of these devices for broadband excitation and focuses purely on the resonant response.

This paper experimentally analysis the power responsiveness of a plain micro-cantilever (MC), a MC with 2 mg added end mass and a MC with 5 mg added end mass. Both the single frequency resonant response as well as the white noise response were investigated. A numerical model based on beam theory and piezoelectric strain-to-charge transduction model was constructed and used to verify the experimental observation.

2. Apparatus

The devices were fabricated by a 0.5 μm aluminium nitride (AlN) on 10 μm doped silicon (Si) process using the material stack shown in figure 1. A cantilever beam of 5 mm length and 2 mm width, as shown in figure 2 was employed.

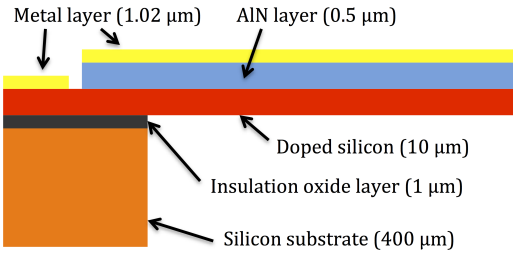

Figure 1. Stack of material used to fabricate the MEMS AlN-on-Si cantilever harvester prototypes.

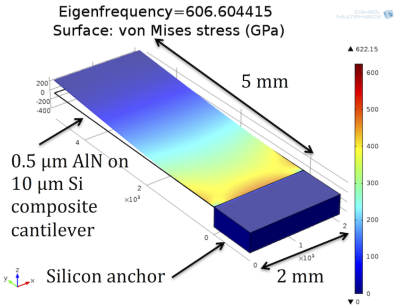

Figure 2. Plain cantilever, fn ∼600 Hz.

Additional mass was added (post fabrication) to the free end of the cantilever using a non-conductive adhesive as shown in figure 3. The mass blocks were made from lead-based solder wire for its high mass density. Using shifts in the natural frequency, beam theory equations and COMSOL simulation fits, the approximate value of the added mass were estimated.

The experimental setup mounted on top of a mechanical shaker is shown in figure 4. Experimentally matched optimal resistive loads were connected in parallel for each variation of the micro-cantilevers: MC0, MC2 and MC5. The central base of the chip carrier was machined to accommodate large travel (±5 mm) in order to prevent premature saturation as a result of physical limits imposed by the package.

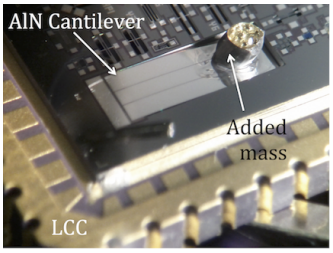

Figure 3. Photograph of micro-cantilever with added solder mass near the free end.

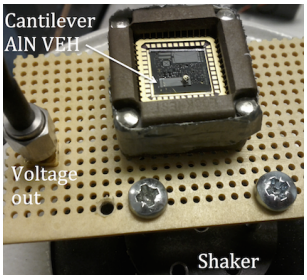

Figure 4. Photograph of the experimental setup on a mechanical shaker.

3. Model

To verify the experimental data measured, a MATLAB numerical model (figure 5) was constructed using the various established equations associated with a classical second order mass-spring-damper resonator (equation 1) when subjected to a periodic mechanical forcing, beam theory for extracting the dynamic bending strain value for a given deflection (equation 2) and the piezoelectric transducer model based on the mechanical strain-induced-charge generation (equation 3). The generated charge can then be assumed as a power source across an impedance equivalent to the capacitance of the piezoelectric layer (equation 4).

$$\ddot{x} + 2\zeta\omega\dot{x} + \omega^2 x + \mu x^3 = A\omega^2 \cos(\omega_0 t) \tag{1}$$

where, x is the displacement or deflection at the free end of the cantilever resonator, ζ is the damping ratio, μ is the Duffing coefficient, ω is the excitation frequency, ω_0 is the natural frequency, A is the excitation displacement, and t is the time domain.

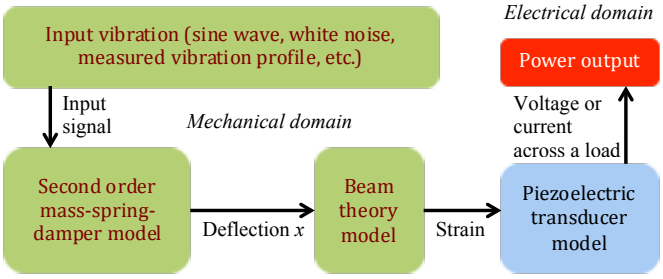

Figure 5. Overview of the MATLAB numerical model used to predict the power output for piezoelectric-on-substrate cantilever designs when subjected to a given vibration profile.

$$\epsilon_y = \frac{3x_{max}h(l-y)}{2l^3} \tag{2}$$

where, ϵ_y is the strain at any arbituary point y along the effective beam length l, x_{max} is the displacement amplitude or the maximum deflection and h is the effective thickness of the beam.

$$q = d_{31}\epsilon_y E w_p l_p \tag{3}$$

where, σ_y is the mechanical stress induced, E and is elastic modulus, q is the total charge generated, and w_p and l_p are the width and length of the active piezoelectric region.

$$P = \frac{\omega h_p q^2}{\varepsilon_0 \varepsilon_r w_p l_p} \tag{4}$$

where, P is the power, ω is the frequency, ε_0 is the permittivity of free space and ε_r is the dielectric constant of the piezo material and h_p, w_p and l_p are the thickness, width and length of the piezo-layer.

4. Result

The characteristics and performance of the three prototype iterations are summarised in table 1. The peak attainable power from the device increased with larger values of added mass, while the acceleration levels required to attain this power level decreased as expected. Driving the cantilevers beyond these acceleration levels yielded either little observable power increase or resulted in failure.

Table 1. The peak attainable power at the required acceleration for the micro-cantilevers.

Device	Added mass (mg)	Frequency (Hz)	Attainable power (μW)	Saturation acceleration (ms^{-2})
MC0	0	577	0.70	70
MC2	2	129	1.90	7
MC5	5	80	2.56	3

Figure 6 illustrates the power output per drive acceleration for the three devices. While a relatively linear relationship can be seen for the plain cantilever MC0, both MC2 and MC5 experienced diminishing returns at higher acceleration levels. The power level at which this deviation from linearity onset are all approximately in the order of few hundreds of nano-watts

to a micro-watt. Additionally, MC2 and MC5 demonstrated appreciable Duffing nonlinearities in the form of spring softening (figure 7), even at relatively low acceleration levels. The unloaded MC0 on the other hand, exhibited a predominantly linear resonant peak within the scanned acceleration range.

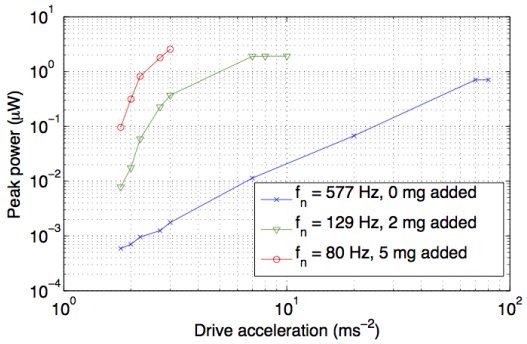

Figure 6. Power response per acceleration for 3 devices with varying added mass.

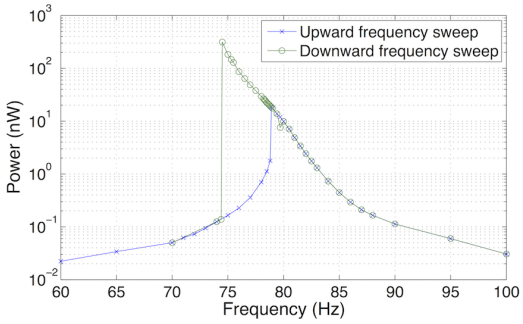

Figure 7. Frequency domain power response for MC5 when driven at 2 ms^{-2}.

The experimental measurements are compared against the numerically simulated results in table 2. Damping ratios for the numerical model of each device configuration was estimated from the measured half power bandwidth and the natural frequency of each prototype. Overall, the model deviation, for the first resonant mode, from the experimental measurement was within ±10% in terms of the power output across a matched impedance.

Table 2. Numerical model deviation from the experimental results for the first resonant mode.

Device	Acceleration (ms^{-2})	Recorded power (μW)	Simulated power (μW)	Deviation (%)
MC0	70	0.70	0.77	+10
MC2	7	1.90	1.86	−2.1
MC5	3	2.56	2.62	+2.3

The cantilever with 5 mg added mass was also subjected to varying levels of band-limited white noise vibration with bandwidths ranging from 10 Hz to 2 kHz. Typical time domain output voltage characteristics of the harvester from amplitudes of 1 g and 4 g are shown in figure 8, which yielded average power outputs of 30.83 nW and 123.32 nW respectively. Figure 9 further details the experimentally measured and simulated peak and average power response of this device from the band-limited white noise. Experimentally, peak instantaneous power in excess of 1 μW was only attainable beyond 2 g of white noise, whereas single frequency resonant response just required ∼2.5 ms^{-2}. Detailed results are presented in table 3.

While the model developed here does not consider higher resonant modes, the first resonant mode dominates the power response. This is primarily due to the partial strain-charge cancellation experienced by the piezoelectric layer at these higher resonant modes when opposing strain gradients co-exist from twists or multiple curvatures. For instance, COMSOL simulation reveals that MC5 has a shear mode at ∼400 Hz and the second transverse mode at ∼1 kHz, where both possess opposing strain gradients.

Therefore, the higher average response amplitude from the experimental prototype towards wide-band excitation, as illustrated by figure 9, is expected; since higher vibrational modes are

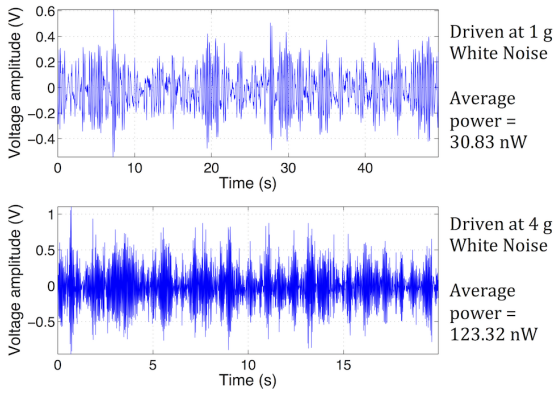

Figure 8. Voltage response from white noise (10 Hz to 2 kHz) of 1 g and 4 g for MC5.

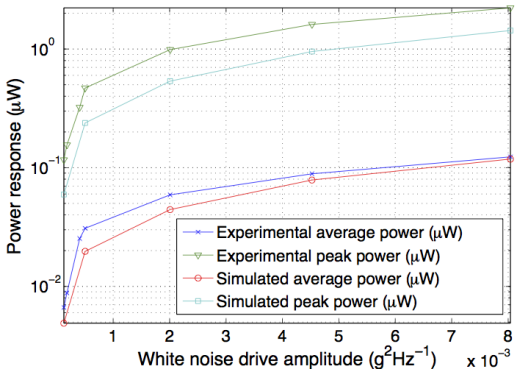

Figure 9. Power response from white noise (10 Hz to 2 kHz) for MC5.

Table 3. Numerical model deviation from the experimental result of MC5 for a band-limited white noise excitation of bandwidth 10 Hz to 2 kHz.

Acc. (g)	Average power (μW) Experimental	Numerical	Deviation (%)	Peak power (μW) Experimental	Numerical	Deviation (%)
0.5	0.007	0.005	-28.6	0.116	0.06	-48.3
1	0.031	0.02	-35.5	0.469	0.238	-49.3
2	0.059	0.044	-25.4	0.988	0.536	-45.7
3	0.089	0.079	-11.2	1.61	0.953	-40.8
4	0.123	0.118	-4.1	2.22	1.43	-35.6

reduced to off-resonant response in the numerical simulation. However, the difference is still well within an order of magnitude, with model deviation varying from -4.1% to -35.5% for the scanned amplitude range. The model deviation from the instantaneous power peaks is slightly more significant, but remains relatively consistent, ranging from -35.7% to -49.2%.

Conclusion

Numerical models and experimental prototypes for AlN-on-Si cantilevers with varying added end mass were developed and investigated. While the first resonant mode response yielded a peak attainable 2.56 μW at 3 ms^{-2} of acceleration for an iteration with 5 mg of added end mass, the same prototype only yielded 123 nW of average power and 2.22 μW of peak instantaneous power when subjected to band-limited white noise (10 Hz to 2 kHz) of 4 g. The model deviations from the measurements were either small or relatively consistent. Future work involves further model validation and improvement towards white noise and broadband excitations by including the response of higher orders of resonance. The model can in turn be used as an optimisation tool for designing for a given vibration profile representative of a specific application.

References

[1] A. Erturk and D. Inman, 2011, *Piezoelectric energy harvesting*, New Delhi, India: Wiley.
[2] M. Renaud, K. Karakaya, T. Sterken, P. Fiorini, C.V. Hoof and R. Puers, 2008, *Sens. Actuators A*, **145-146**, pp. 380-386.
[3] R. Andosca, T.G. McDonald, V. Genova, S. Rosenberg, J. Keating, C. Benedixen and J. Wu, 2012, *Sens. Actuators A*, **178**, pp. 76-87.